

# $\beta$ -(Ethynylbenzoic acid)-substituted push-pull porphyrins: DSSC dyes prepared by a direct palladium-catalyzed alkynylation reaction†

Cite this: *Chem. Commun.*, 2013, **49**, 9164

Received 28th June 2013,  
Accepted 12th August 2013

DOI: 10.1039/c3cc44847a

www.rsc.org/chemcomm

Masatoshi Ishida,<sup>ab</sup> Deasub Hwang,<sup>ac</sup> Young Bean Koo,<sup>a</sup> Jooyoung Sung,<sup>a</sup>  
Dong Young Kim,<sup>c</sup> Jonathan L. Sessler\*<sup>ad</sup> and Dongho Kim\*<sup>a</sup>

The palladium-catalyzed oxidative alkynylation of  $\beta$ -borylated porphyrins allows for concise preparation of push-pull structured ethynylbenzoic acid porphyrin derivatives. The resulting  $\beta$ -singly- and doubly-substituted porphyrin dyes are regarded as isomeric derivatives of the corresponding *meso*-substituted reference systems, and were found to give rise to nearly equal power conversion efficiencies when analyzed in DSSCs.

Porphyrins are an important family of organic chromophores that has attracted attention as photosensitizers in TiO<sub>2</sub>-based dye-sensitized solar cells (DSSCs).<sup>1</sup> Relatively high photo-voltaic efficiencies have been demonstrated in DSSCs based on “push(donor)–pull(acceptor)” structured porphyrin dyes.<sup>2</sup> A key feature of successful push-pull porphyrin sensitizers is the unidirectional “D– $\pi$ –A” arrangement of the electron donating substituent, typically a diarylamine, and the electron-acceptor, an ethynylbenzoic acid anchoring group, across the 5- and 15-(*meso*) positions of the porphyrin core. A breakthrough in the world of DSSCs was attained recently, wherein a power conversion efficiency ( $\eta$ ) of 11.9% was obtained using porphyrin-sensitized cells of this general structure (*viz.*, **YD2-o-C8**; Chart 1) and a cobalt-based redox electrolyte system.<sup>3</sup> The outstanding results obtained using **YD2-o-C8** provide an incentive to develop synthetic methods that would allow a range of “D– $\pi$ –A<sub>2</sub>” porphyrin sensitizers to be prepared such that the effect of structural modification on functional efficiency can be probed in detail. Of particular interest within the cadre of this generalized approach would be elucidating the effect of  $\beta$ -pyrrolic *vs.* *meso*-substitution

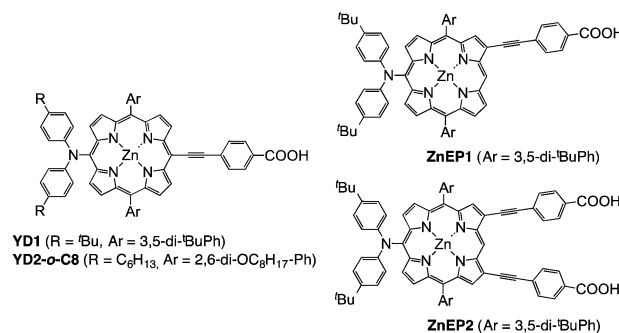


**Chart 1** Molecular structures of **YD<sub>n</sub>** series and our porphyrins, **ZnEP<sub>n</sub>** used in this study; *n* = 1 and 2.

of acceptor subunits. In previous work, we reported the preparation of doubly  $\beta$ -vinylogous-linked porphyrins where the alkenyl spacer was thought to play a role in improving the overall efficiency by mediating effective charge separation.<sup>4</sup> In the present study, we report a new set of porphyrin-based photosensitizers prepared through a direct palladium-catalyzed alkynylation reaction of  $\beta$ -borylated porphyrins with various terminal alkyne derivatives. It was expected that the presence of the rigid C $\equiv$ C triple-bond and the resulting enhancement of electronic communication through the  $\beta$ -positions would facilitate effective electron injection into the conduction band of the TiO<sub>2</sub>. As detailed below, the DSSC efficiencies of  $\beta$ -(4-ethynylbenzoic acid)-substituted derivatives (singly- and doubly-substituted; **ZnEP1** and **ZnEP2**, respectively) proved to be nearly equal to the corresponding *meso*-linked derivative (*i.e.*, **YD1**<sup>5</sup>) as measured using a sensitized TiO<sub>2</sub> photoelectrode (Chart 1).

The iridium(i) catalyst-assisted borylated porphyrins (**1a**: mono-boryl and **1b**: di-boryl porphyrins) are potentially useful precursors for direct alkynyl coupling reactions.<sup>6</sup> We thus sought to effect the cross-coupling between the porphyrin borylester derivative (**1a**) and the readily available terminal acetylene derivative **2b** to access the corresponding zinc porphyrin **ZnEP<sub>n</sub>** (*n* = 1 or 2). To date, there have been few studies involving the oxidative alkynylation reactions of analogous borylated precursors, although it was found that Pd/Ag<sup>7</sup> or Cu catalysts<sup>8</sup> were not effective when tested with

<sup>a</sup> Department of Chemistry, Yonsei University, Seoul, 120-749, Korea.

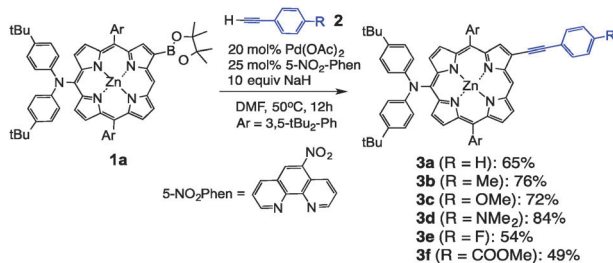
E-mail: dongho@yonsei.ac.kr

<sup>b</sup> Education Center for Global Leaders in Molecular Systems for Devices, Kyushu University, Fukuoka 819-0395, Japan

<sup>c</sup> Optoelectronic Materials Lab, IMCM, Korea Institute of Science and Technology, Seoul 130-650, Korea

<sup>d</sup> Department of Chemistry & Biochemistry, University of Texas at Austin, Texas 78712-1224, USA. E-mail: sessler@cm.utexas.edu

† Electronic supplementary information (ESI) available: Synthetic experimental procedure, characterization data, a proposed reaction mechanism, spectroscopic data, calculations, and results obtained from test DSSC experiments. See DOI: 10.1039/c3cc44847a



**Scheme 1** Palladium-catalyzed alkylation of **1** with various terminal alkyne derivatives **2**.

large  $\pi$ -conjugated porphyrins (cf. ESI<sup>†</sup>). After extensive screening of reaction conditions, we found that mild palladium-catalyzed aerobic oxidative coupling of  $\beta$ -borylated porphyrins, **1** with various terminal alkynes, **2** allows access to the desired cross-linked products (**3**) in satisfactory yields (Scheme 1 and Fig. S1, ESI<sup>†</sup>). Electron deficient alkynes (e.g., **2e** and **2f**) proved to be less reactive compared to electron rich ones (e.g., **2c** and **2d**); however, a variety of terminal alkynes were tolerated. The procedure was sufficiently robust that the doubly-(methyl ethynylbenzoate)-substituted derivative (**3g**) could be isolated in 15% yield starting from the diborylated derivative (**1b**).<sup>9</sup> A proposed mechanism for the coupling reaction is provided in the ESI<sup>†</sup> (cf. Scheme S1).<sup>10</sup>

The isolated methyl ester derivatives (**3f** and **3g**) could be easily hydrolyzed under basic conditions. The final products, **ZnEP1** and **ZnEP2**, were characterized by <sup>1</sup>H- and <sup>13</sup>C-NMR spectroscopy and high resolution FAB mass spectrometry (ESI<sup>†</sup>).

The light-harvesting ability of **ZnEP1** and **ZnEP2** was confirmed by steady-state absorption spectroscopy in CH<sub>2</sub>Cl<sub>2</sub> (Fig. 1a). These two **ZnEPns** exhibited Soret bands and Q-bands in 400–500 and 550–700 nm spectral ranges, respectively, which were broadened and red-shifted as the number of  $\beta$ -linkages increased ( $\lambda_{\text{max}} = 422$  nm;  $\epsilon = 1.59 \times 10^5 \text{ M}^{-1} \text{ cm}^{-1}$  for **ZnEP1** and  $\lambda_{\text{max}} = 439$  nm;  $\epsilon = 1.31 \times 10^5 \text{ M}^{-1} \text{ cm}^{-1}$  for **ZnEP2**).<sup>11</sup> The absorption spectra of **ZnEPn** are also characterized by a shoulder at 450–500 nm, which is not present in the spectrum of the *meso*-linked analogue **YD1**.<sup>5</sup> The spectral features are thought to reflect the electronic interaction between the porphyrin macrocyclic core and the  $\beta$ -ethynylaryl substituents resulting in an effective extension in the overall  $\pi$ -conjugation.

In accord with what was seen in the absorption spectral studies, the fluorescence maxima of **ZnEP1** and **ZnEP2** also shift to lower energy as the degree of substitution increases (Fig. 1b).<sup>11</sup> The zero-zero excitation energies ( $E_{0-0}$ ) are estimated to be 1.91 and 1.85 eV for **ZnEP1** and **ZnEP2**, respectively (Table S1, ESI<sup>†</sup>).

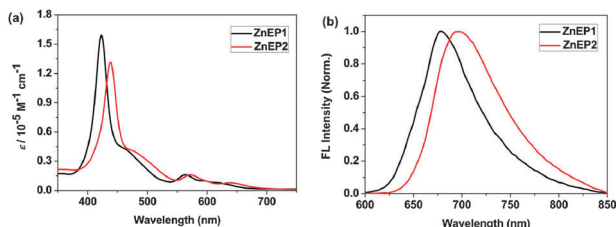


**Fig. 1** (a) Steady-state absorption and (b) fluorescence spectra of **ZnEP1** (black) and **ZnEP2** (red) recorded in CH<sub>2</sub>Cl<sub>2</sub>. Excitation was made in the Soret band.

The time-resolved fluorescence decay profiles of **ZnEP1** and **ZnEP2** recorded in CH<sub>2</sub>Cl<sub>2</sub> could fit well as a single exponential decay with a time constant of 1.46 and 1.35 ns, respectively (Fig. S3, ESI<sup>†</sup>). It is worth noting that the observed excited state lifetimes are longer than the electron injection rate (meaning deactivation is unlikely to compete with the electron injection into TiO<sub>2</sub>).<sup>12</sup>

The electrochemical properties of **ZnEP1** and **ZnEP2** were investigated by cyclic voltammetry in THF containing 0.1 M tetra-*n*-butylammonium hexafluorophosphate (TBAPF<sub>6</sub>) as the supporting electrolyte (Table S1, ESI<sup>†</sup>). The oxidation potentials for **ZnEP1** and **ZnEP2** were determined to be approximately 1.0 V (vs. NHE), which is comparable to those of the other diarylamine-substituted porphyrins.<sup>5,13</sup> The injection potential ( $E_{\text{ox}}^*$ ) was evaluated by subtracting the excitation energy ( $E_{0-0}$ ) from the oxidation potential ( $E_{\text{ox}}$ ) of the porphyrins, giving values of  $-1.14$  V and  $-1.08$  V (vs. NHE) for **ZnEP1** and **ZnEP2**, respectively. Based on the optical and electrochemical parameters, the driving force for electron injection ( $\Delta G_{\text{inj}}$ ) from the porphyrin excited state to the conduction band of the TiO<sub>2</sub> ( $-0.5$  V vs. NHE) and the regeneration ( $\Delta G_{\text{reg}}$ ) of the porphyrin radical cation by the Co(II/III) redox couple ( $+0.56$  V vs. NHE) for DSSCs built from **ZnEP1** and **ZnEP2** are expected to be thermodynamically favoured ( $\Delta G < 0$ ).

Density functional theory (DFT) calculations were carried out at the B3LYP/6-31G(d) level to gain insight into the charge transfer character of the dyes (Fig. S4 and Table S3, ESI<sup>†</sup>). The overall electron distribution pattern of the two **ZnEPns** of this study is essentially similar to that of **YD1**.<sup>5</sup> Despite the lower molecular symmetry of **ZnEP1** compared to that of **YD1**, the characteristic orbital densities and phases are retained. Specifically, **ZnEP1** and **ZnEP2** were predicted to be dipolar in nature, which is expected to facilitate efficient and rapid electron injection into the CB of TiO<sub>2</sub>, as seen in other push-pull porphyrin derivatives.<sup>2</sup> The time-dependent DFT analyses of **ZnEP1** and **ZnEP2** were also consistent with the experimental absorption spectra (Fig. S5, ESI<sup>†</sup>).

To clarify the effect of the number (1 vs. 2) and orientation ( $\beta$ - vs. *meso*-) of the linkage, DSSCs were fabricated using **ZnEPns** as photosensitizers and mesoporous anatase TiO<sub>2</sub> spheres (diameter  $\sim 600$  nm) prepared by an electrostatic spray method.<sup>14</sup> The photovoltaic properties of these two porphyrins were then investigated under AM 1.5 irradiation conditions ( $100 \text{ mW cm}^{-2}$ ) using a Co(bpy)<sub>3</sub>-based electrolyte.<sup>15</sup> The photocurrent density–voltage ( $J$ - $V$ ) curves of the sandwich type cells sensitized with **ZnEP1** and **ZnEP2** in the presence of 2 equiv. of chenodeoxycholic acid (CDCA) as a co-adsorbent allowed the short circuit photocurrent density ( $J_{\text{SC}}$ ,  $\text{mA cm}^{-2}$ ), open circuit voltage ( $V_{\text{OC}}$ , V), and fill factor (FF) to be calculated. This yielded an overall conversion efficiency ( $\eta$ ) of 5.9% for **ZnEP1** and 4.0% for **ZnEP2** according to the equation,  $\eta = J_{\text{SC}} \times V_{\text{OC}} \times \text{FF}$  (Fig. 2a and Table 1).

The efficiency of the doubly  $\beta$ -ethynylphenyl-substituted **ZnEP2** used in the present study proved to be inferior to that of singly-substituted **ZnEP1** as manifest in the lower  $J_{\text{SC}}$  value. The photocurrent action spectra of the **ZnEP1**-sensitizer cell exhibited a maximum incident photon-to-current efficiency (IPCE) of 54.5%

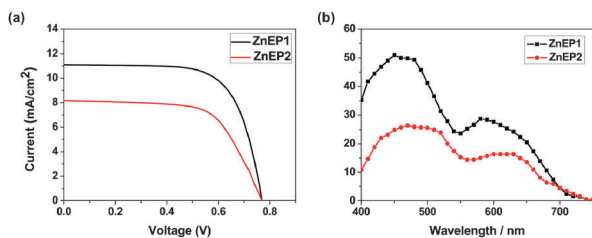


**Fig. 2** (a) Current–voltage characteristics and (b) action spectra at incident photon-to-current (IPCE) conversion efficiencies of DSSCs sensitized by **ZnEP1** (black) and **ZnEP2** (red). Conditions: [Co(bpy)<sub>3</sub>]<sup>2+</sup> based electrolyte in CH<sub>3</sub>CN and AM 1.5 under simulated solar light irradiation (100 mW cm<sup>-2</sup>).

**Table 1** Photovoltaic performances of **ZnEPn**-sensitized cells<sup>a</sup>

Dyes	$J_{SC}/\text{mA cm}^{-2}$	$V_{OC}/\text{V}$	FF	$\eta/\%$
<b>ZnEP1</b>	11.1	0.77	0.69	5.9
<b>ZnEP2</b>	8.2	0.77	0.64	4.0
<b>YD1</b> <sup>b</sup>	12.7	0.71	0.68	6.2

<sup>a</sup> Under AM 1.5 illumination (power 100 mW cm<sup>-2</sup>) with an active area of 0.25 cm<sup>2</sup> and a TiO<sub>2</sub> thickness of 13 μm. As a reference, the overall efficiency of N3 sensitized solar cells was determined;  $J_{SC} = 15.3 \text{ mA cm}^{-2}$ ,  $V_{OC} = 0.78 \text{ V}$ , FF = 0.66, and  $\eta = 7.7\%$ . <sup>b</sup> See ref. 5b.

at 450 nm that is also larger than in cells built up from **ZnEP2** (27.3% at 470 nm) (Fig. 2b). This difference matched the absorption spectral features of the corresponding porphyrins adsorbed on the electrodes (Fig. S6, ESI<sup>†</sup>).

The photocurrent density of DSSCs is related to the efficiencies of (i) light harvesting (LHE), (ii) charge injection ( $\phi_{inj}$ ), and (iii) charge collection ( $\eta_{col}$ ).<sup>16</sup> Among these factors, the LHE defined as  $LHE = 1 - 10^{-\epsilon\Gamma}$  (where  $\epsilon$  is the molar extinction coefficient of the dye and  $\Gamma$  is the molar concentration of the dye per projected surface area of the film) is thought to be dominant in accounting for the photocurrent generated by the cells prepared using **ZnEPn** of this study. Considering the similar absorption spectral features of the dyes, the larger  $\Gamma$  value of **ZnEP1** ( $1.2 \times 10^{-7} \text{ mol cm}^{-2}$ ) as determined on our TiO<sub>2</sub> electrode serves to enhance the overall efficiency of this porphyrin relative to **ZnEP2** ( $\Gamma = 4.4 \times 10^{-8} \text{ mol cm}^{-2}$ ).

The dye aggregates on the surface are known to be one of the factors accounting for low efficiency.<sup>13a,17</sup> On this basis we consider it possible that the tilted dye geometry of **ZnEP2** serves to accelerate the back electron transfer process (Fig. S7, ESI<sup>†</sup>). In addition, the dihedral angle between the porphyrin core and the acceptor ethynylphenyl rings is larger in **ZnEP2** than in **ZnEP1** based on the optimized structures (Fig. S8, ESI<sup>†</sup>; 17.4° vs. 0.7°, respectively). This may disrupt the effective electronic communication through the  $\beta$ -ethynylphenyl  $\pi$ -bridges. To an extent this is true, it would help to rationalize the relatively poor power conversion efficiency seen for the doubly-bridged system.

In summary, we have demonstrated the use of a direct palladium-catalyzed oxidative alkynylation reaction of  $\beta$ -borylated porphyrins to obtain  $\beta$ -ethynylphenyl-substituted porphyrin derivatives. This has allowed us to obtain new alternative porphyrin-based sensitizers, **ZnEPn** for DSSCs. The photophysical and electrochemical properties of two **ZnEPns** were investigated and proved to be similar to those of a *meso*-substituted control system,

**YD1**, confirming the viability of the present substitution strategy. It was also found that the power conversion efficiency of the monosubstituted **ZnEP1** is superior to that of its doubly functionalized **ZnEP2**, leading us to suggest that further design optimization could produce yet-improved systems.

This work was supported by the Global Frontier R&D Program on Center for Multiscale Energy System funded by the National Research Foundation under the Ministry of Science, ICT & Future, Korea (2012-8-2081; D.K.) and the U.S. NSF (CHE-1057904; J.L.S.).

## Notes and references

- (a) M. K. Panda, K. Ladomenou and A. G. Coutsolelos, *Coord. Chem. Rev.*, 2012, **256**, 2601; (b) X.-F. Wang and H. Tamiaki, *Energy Environ. Sci.*, 2010, **3**, 94.
- L.-L. Li and E. W.-G. Diau, *Chem. Rev. Soc.*, 2013, **42**, 291.
- A. Yella, H. W. Lee, H. N. Tsao, C. Yi, A. K. Chandiran, M. K. Nazeeruddin, E. W.-G. Diau, C. Y. Yeh, S. M. Zakeeruddin and M. Grätzel, *Science*, 2011, **334**, 629.
- M. Ishida, S. W. Park, D. Hwang, Y. B. Koo, J. L. Sessler, D. Y. Kim and D. Kim, *J. Phys. Chem. C*, 2011, **115**, 19343.
- (a) C.-W. Lee, H.-P. Lu, C.-M. Lan, Y.-L. Huang, Y.-R. Liang, W.-N. Yen, Y.-C. Liu, Y.-S. Lin, E. W.-G. Diau and C.-Y. Yeh, *Chem.-Eur. J.*, 2009, **15**, 1403; (b) C.-P. Hsieh, H.-P. Lu, C.-L. Chiu, C.-W. Lee, S.-H. Chuang, C.-L. Mai, W.-N. Yen, S.-J. Hsu, E. W.-G. Diau and C.-Y. Yeh, *J. Mater. Chem.*, 2010, **20**, 1127.
- H. Hata, H. Shinokubo and A. Osuka, *J. Am. Chem. Soc.*, 2005, **127**, 8264.
- (a) G. Zou, J. Zhu and J. Tang, *Tetrahedron Lett.*, 2003, **44**, 8709; (b) F. Yang and Y. Wu, *Eur. J. Org. Chem.*, 2007, 3476; (c) X. Nie, S. Liu, Y. Zong, P. Sun and J. Bao, *J. Organomet. Chem.*, 2011, **696**, 1570.
- (a) C. Pan, F. Luo, W. Wang, Z. Ye and J. Cheng, *Tetrahedron Lett.*, 2009, **50**, 5044; (b) M. Wu, J. Mao, J. Guo and S. Ji, *Eur. J. Org. Chem.*, 2008, 4050; (c) T. Yasukawa, H. Miyamura and S. Kobayashi, *Org. Biomol. Chem.*, 2011, **9**, 6208.
- The reduced overall yield is ascribed in part to the partial hydrolysis of the methyl ester product (**3g**) formed under the reaction conditions. Unfortunately, in our hands the polar hydrolyzed product could not be isolated *via* silica gel column chromatography.
- C. Adamo, C. Amatore, I. Ciofini, A. Jutand and H. Lakmini, *J. Am. Chem. Soc.*, 2006, **128**, 6829.
- Optical data for the unfunctionalized porphyrin (**4**) are also given in Fig. S2 (ESI<sup>†</sup>) for the purpose of comparison.
- Electron injection from the excited state of a sensitized dye to the TiO<sub>2</sub> surface has been reported to take place on a time scale of  $10^{12}$ – $10^{13} \text{ s}^{-1}$ . See, Y. Tachibana, S. A. Haque, I. P. Mercer, J. R. Durrant and D. R. Klug, *J. Phys. Chem. B*, 2000, **104**, 1198.
- (a) S. Mathew, H. Iijima, Y. Toude, T. Umeyama, Y. Matano, S. Ito, N. V. Tkachenko, H. Lemmetyinen and H. Imahori, *J. Phys. Chem. C*, 2011, **115**, 14415; (b) N. M. Reddy, T.-Y. Pan, Y. C. Rajan, B.-C. Guo, C.-M. Lan, E. W.-G. Diau and D.-Y. Yeh, *Phys. Chem. Chem. Phys.*, 2013, **15**, 8409.
- (a) D. Hwang, H. Lee, S.-Y. Jang, S. M. Jo, D. Kim, Y. Seo and D. Y. Kim, *ACS Appl. Mater. Interfaces*, 2011, **3**, 2719; (b) D. Hwang, D. Y. Kim, S.-Y. Jang and D. Kim, *J. Mater. Chem. A*, 2013, **1**, 1228; (c) D. Hwang, H. Y. Seo, D. Kim, S. M. Jo and D. Y. Kim, *J. Mater. Chem. A*, 2013, **1**, 1359.
- S. M. Feldt, E. A. Gibson, E. Gabrielsson, L. Sun, G. Boschloo and A. Hagfeldt, *J. Am. Chem. Soc.*, 2010, **132**, 16714.
- M. K. Nazeeruddin, A. Kay, R. Rodicio, R. Humphry-Baker, E. Müller, P. Liska, N. Vlachopoulos and M. Grätzel, *J. Am. Chem. Soc.*, 1993, **115**, 6382.
- (a) H. Imahori, S. Kang, H. Hayashi, M. Haruta, H. Kurata, S. Isoda, S. E. Canton, Y. Infahsaeng, A. Kathiravan, T. Pascher, P. Chábera, A. P. Yartsev and V. Sundström, *J. Phys. Chem. A*, 2011, **115**, 3679; (b) A. Kira, Y. Matsubara, H. Iijima, T. Umeyama, Y. Matano, S. Ito, M. Niemi, N. V. Tkachenko, H. Lemmetyinen and H. Imahori, *J. Phys. Chem. C*, 2010, **114**, 11293; (c) C.-L. Wang, C.-M. Lan, S.-H. Hong, Y.-F. Wang, T.-Y. Pan, C.-W. Chang, H.-H. Kuo, M.-Y. Kuo, E. W.-G. Diau and C.-Y. Lin, *Energy Environ. Sci.*, 2012, **5**, 6933; (d) Z. Ning, Y. Fu and H. Tian, *Energy Environ. Sci.*, 2010, **3**, 1170.